Bull. Mater. Sci. (2022)45:108
https://doi.org/10.1007/s12034-022-02688-3

Electronic structure of two-dimensional-layered $PbTiO_3$ perovskite crystal: an extended tight-binding study based on DFT

FATIH AHMET CELIK
Faculty of Arts and Sciences, Physics Department, Bitlis Eren University, 13000 Bitlis, Turkey
For correspondence (facelik@beu.edu.tr)

MS received 13 December 2021; accepted 9 February 2022

Abstract. The electronic structure of bulk and slab $PbTiO_3$ perovskite crystal for different layers are investigated using extended-tight binding calculations (GFN1-xTB) with self-consistent charge calculations based on density functional theory. The band structure is calculated for bulk $PbTiO_3$, and the bandgap is determined as 4.3 eV which is in good agreement with experimental data. The bandgaps of slab $PbTiO_3$ for (001) surfaces with five layers from $n = 2$ to $n = 6$ are calculated as 2.35, 2.49, 2.65, 2.77 and 2.83 eV, respectively. These results are compared with previous quantum mechanics calculations. Also, the total and partial density of states for five layers with (001) surface and the surface formation energies of slab $PbTiO_3$ are discussed.

Keywords. $PbTiO_3$; electronic properties; extended tight binding; DFT.

1. Introduction

The $XTiO_3$-type perovskite crystals have recently attracted remarkable interest with many applications in electro-optical devices. Also, they are important materials for numerous high-tech applications, such as high capacity and optical waveguides, and have a wide range of electric and magnetic properties [1–3]. Especially, $XTiO_3$ (X = Ba, Sr, Pb) materials classified into mixed oxides have been known to exhibit interesting electronic, optical and structural characteristics with the development of technology [3–7]. Besides bulk crystal behaviours, experimental measurements show that the slab geometry with a few monolayers thick can display a ferroelectric ordering at two dimensions [8,9]. Many other experimental investigations have presented different stimulating applications of perovskite oxide titanates [10,11]. On the other hand, quantum mechanical calculations based on density functional theory (DFT) have been widely used for information related to the physical properties of these crystals [12–18]. In this context, Meyer *et al* [7] studied plane-wave calculations in DFT by using pseudo-potentials of $PbTiO_3$, $BaTiO_3$ and $SrTiO_3$. Heifets *et al* [12] reported a computational investigation using *ab-initio* calculations for $SrTiO_3$ surfaces. Lazaro *et al* [17] carried out the structural and electronic properties of the $PbTiO_3$ slabs using DFT. Piskunov *et al* [4] examined the electronic structure of the $SrTiO_3$, $BaTiO_3$ and $PbTiO_3$ perovskite crystals and discussed bulk properties with detailed optimization of basis set using *ab-initio* HF and DFT with Hay–Wadt pseudo-protentional. Noor *et al* [2] explored the physical behaviour of $Pb/SnTiO_3$ by using DFT and obtained the optoelectronic and thermoelectric properties using modified Becke–Johnson exchange potential.

However, there is no computational study investigating the electronic properties and surface formation energies of slab $PbTiO_3$, including different layers via extended tight-binding (TB) method based on DFT calculations. Here, extended TB approximation including self-consistent contributions (GFN1-xTB) is new semi-empirical TB method. Furthermore, it provides a high accuracy calculation for all combinations of the periodic table with a wide range of systems [19–21].

This study aims to determine the surface and surface formation energies of slab $PbTiO_3$ by using the extended TB approach, including self-consistent contributions based on the semi-empirical method. Moreover, the effect of the constructed multilayers, which has two interfaces with different layer lengthiness on bandgap for slab $PbTiO_3$ perovskite crystal, was also investigated.

2. Materials and method

2.1 *General GFN1-xTB formalism*

DFT proposed by Kohn and Sham (KS) [22] is an effective method for investigating the physical properties of different systems, such as molecules, atomic clusters and materials. Density-functional tight-binding (DFTB) based on the

Published online: 16 June 2022

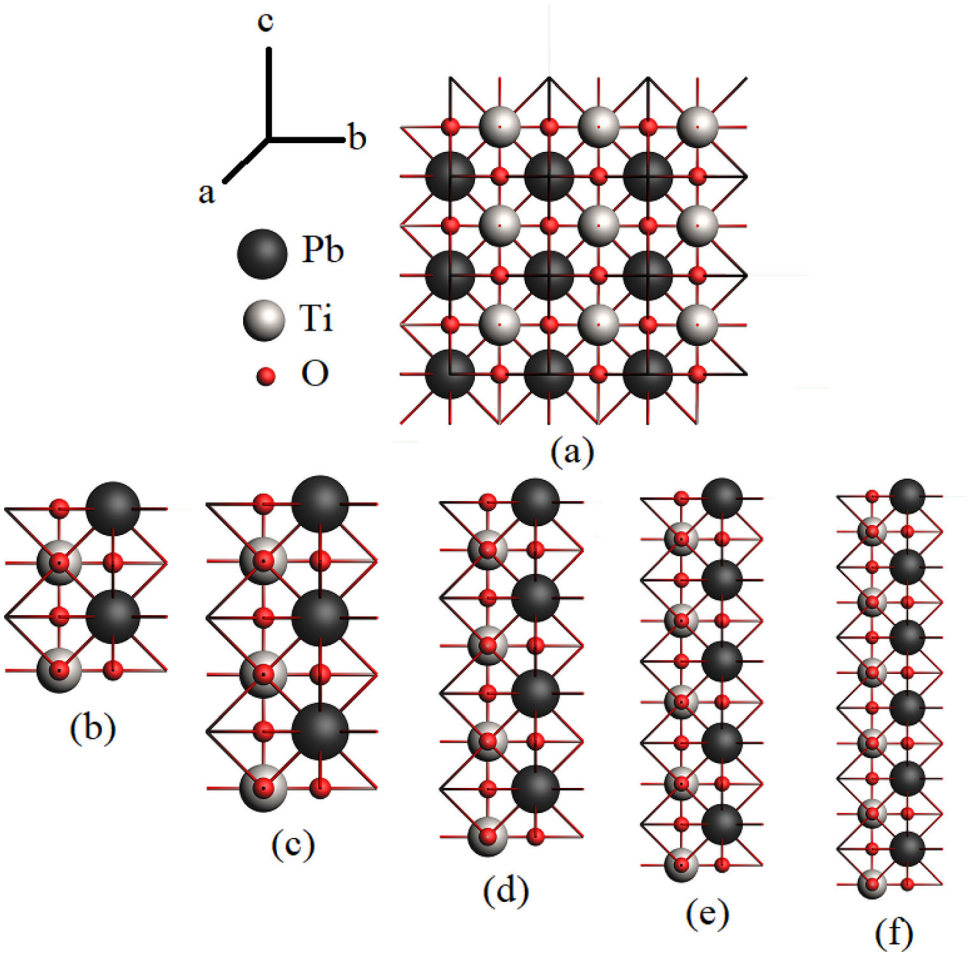

Figure 1. Optimized geometries of $PbTiO_3$: (**a**) bulk structure, (**b**) slab $n = 2$ layer, (**c**) slab $n = 3$ layer, (**d**) slab $n = 4$ layer, (**e**) slab $n = 5$ layer and (**f**) slab $n = 6$ layer.

density functional framework does not require large amounts of empirical parameters [23]. On the other hand, GFN1-xTB is a new extended TB method introduced by Grimme *et al* [20] that provide enough accuracy for geometry optimizations. To the best of our knowledge, xTB does not require the atom-specific parameters when compared to the other semi-empirical code. Although various semi-empirical methods employ minimal atomic orbital basis sets, the GFN1-xTB consists of a minimal basis set of atom centred. In addition, the number of parameters provide a minimum because mainly global parameters are employed.

The total energy expression comprises electronic (el), atom pairwise repulsion (rep), dispersion (disp), and halogen-bonding (XB) terms:

$$E = E_{\mathrm{el}} + E_{\mathrm{rep}} + E_{\mathrm{disp}} + E_{\mathrm{XB}} \tag{1}$$

The electronic energy E_{el} is given by:

$$E_{\mathrm{el}} = \sum_{i}^{\mathrm{occ.}} n_{\mathrm{i}} \langle \varphi_{\mathrm{i}} | H_0 | \varphi_{\mathrm{i}} \rangle + \frac{1}{2} \sum_{A,B} \sum_{l(A)} \sum_{l'(B)} p_{\mathrm{l}}^{\mathrm{A}} p_{\mathrm{l}}^{\mathrm{B}} \gamma_{\mathrm{AB,ll'}} + \frac{1}{3} \sum_{A} \tau_{\mathrm{A}} q_{\mathrm{A}}^{3} - T_{\mathrm{el}} S_{\mathrm{el}}, \tag{2}$$

where φ_{i} is the valence molecular orbitals with occupation numbers n_{i} and H_0 is the zero-order Hamiltonian. $T_{\mathrm{el}}S_{\mathrm{el}}$ is the electronic free energy term [20]. The self-consistent contributions is represented by a second-order term [20,21].

Because GFN1-xTB method covers most of the elements of the periodic table up to $Z = 86$, it is the first TB method that includes a complete parameterization of all the atoms existing in the perovskite-type crystal [24]. Hence, we first practice that the bulk $PbTiO_3$ crystal is geometric optimized and then, the bulk unit cell of the system has been transformed into a slab periodicity construct the (2×2) supercell, which constructed layers (n) in the range of 2–6 for the (001) surface. Finally, the geometries are optimized via the semi-empirical TB method based on GFN1-xTB. The optimized geometries of bulk and slab structures from $n = 2$ to $n = 6$ are shown in figure 1 and information about lattice parameters of bulk and slab with the range between $n = 2$ and $n = 6$ layers are listed in table 1. The computation is carried out using GFN1-xTB in Amsterdam Modeling Suite (AMS) software via DFTB module [25–27]. The maximum force and energy convergence are executed as 0.001 Ha $\mathrm{Å}^{-1}$ and 1×10^{-5} Ha on each atom until the

Table 1. Lattice and layer parameters of bulk and slab $PbTiO_3$.

Bulk		Slab		
Lattice parameters (Å)	Lattice parameters (Å)	Area (Å^2)	Layer lengths (Å)	
$a = 3.64$	$b = 3.64$	13.2	$n = 2$	5.75
$b = 3.64$	$a = 3.64$		$n = 3$	9.27
$b = 3.64$	$\gamma = 90°$		$n = 4$	12.85
$\alpha = 90°$			$n = 5$	16.46
$\beta = 90°$			$n = 6$	20.08
$\gamma = 90°$				

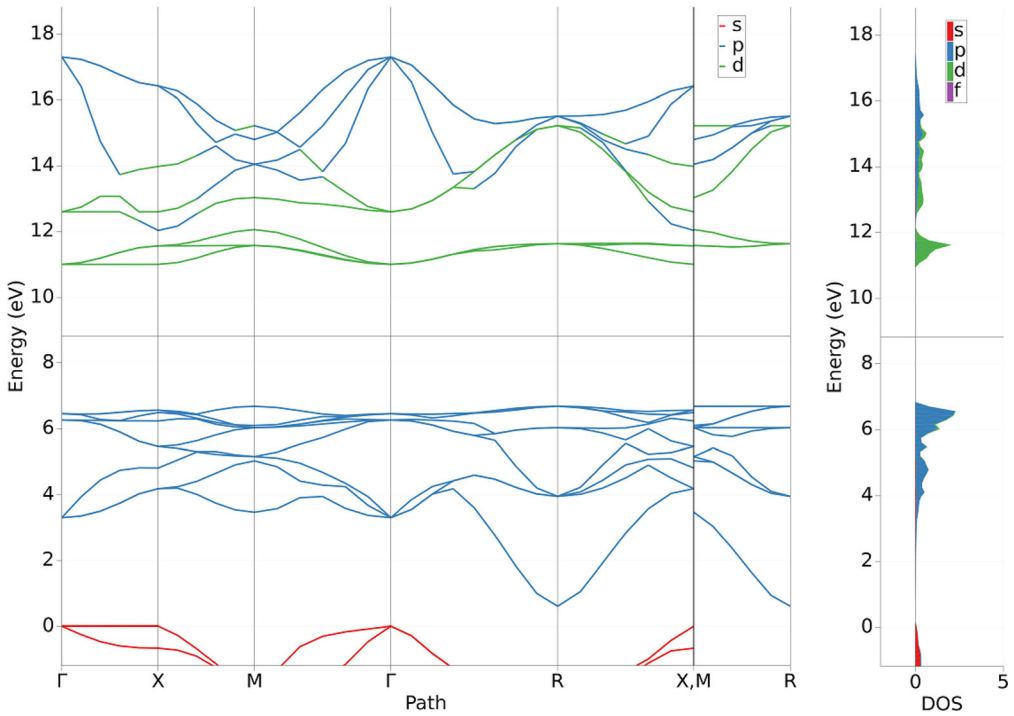

Figure 2. Band structure of bulk $PbTiO_3$ and total DOS.

lattice constants and the atomic positions are relaxed during the geometric optimization process. The stress-energy per atom during the optimized lattice is set up at 5×10^{-5} Ha. The quality of the k-space grid is selected as a good option for the best convergence of calculations. We have used and generated a standard path through the Brillouin zone.

3. Results and discussion

In bulk crystal order, $XTiO_3$-type perovskite crystals exhibit a typical wide-bandgap semiconductor in the range of 3.0 at 4.5 eV [11,17]. The band structure of bulk $PbTiO_3$ is shown in figure 2. Our computations show that the valence band maximum occurred at M path, while the conduction band minimum occurred at the Γ symmetry point in the Brillouin zone which makes an indirect bandgap semiconductor. This indirect bandgap is calculated as 4.3 eV along with the high symmetry directions. This result is in agreement with the experimentally obtained bandgap [7,17]. The detailed total density of states (TDOS) to understand the electronic is also plotted in figure 2, right side. In the valance band and below the Fermi level, the dominant contribution comes from O p-states in the low energy region. Upper the Fermi level, the conduction band is filled with p-states of Pb and 3d-states of Ti. The Pb p-states overlap the Ti-d states in bulk $PbTiO_3$. The calculated total density of states (DOS) curves for five layers with (001) indices of slab $PbTiO_3$ are shown in figure 3a–e. As seen from the figures, the Fermi level locates in the bandgap because of the semiconductor behaviour of the system. Below Fermi energy, there are dense DOS curves with three main regions located at around −5 and −16 eV. On the other hand, the peaks of DOS increase gradually with the increasing of slab layers. The electronic contribution to DOS increases as the atoms forming the slab increase. The partial DOS of slab $PbTiO_3$

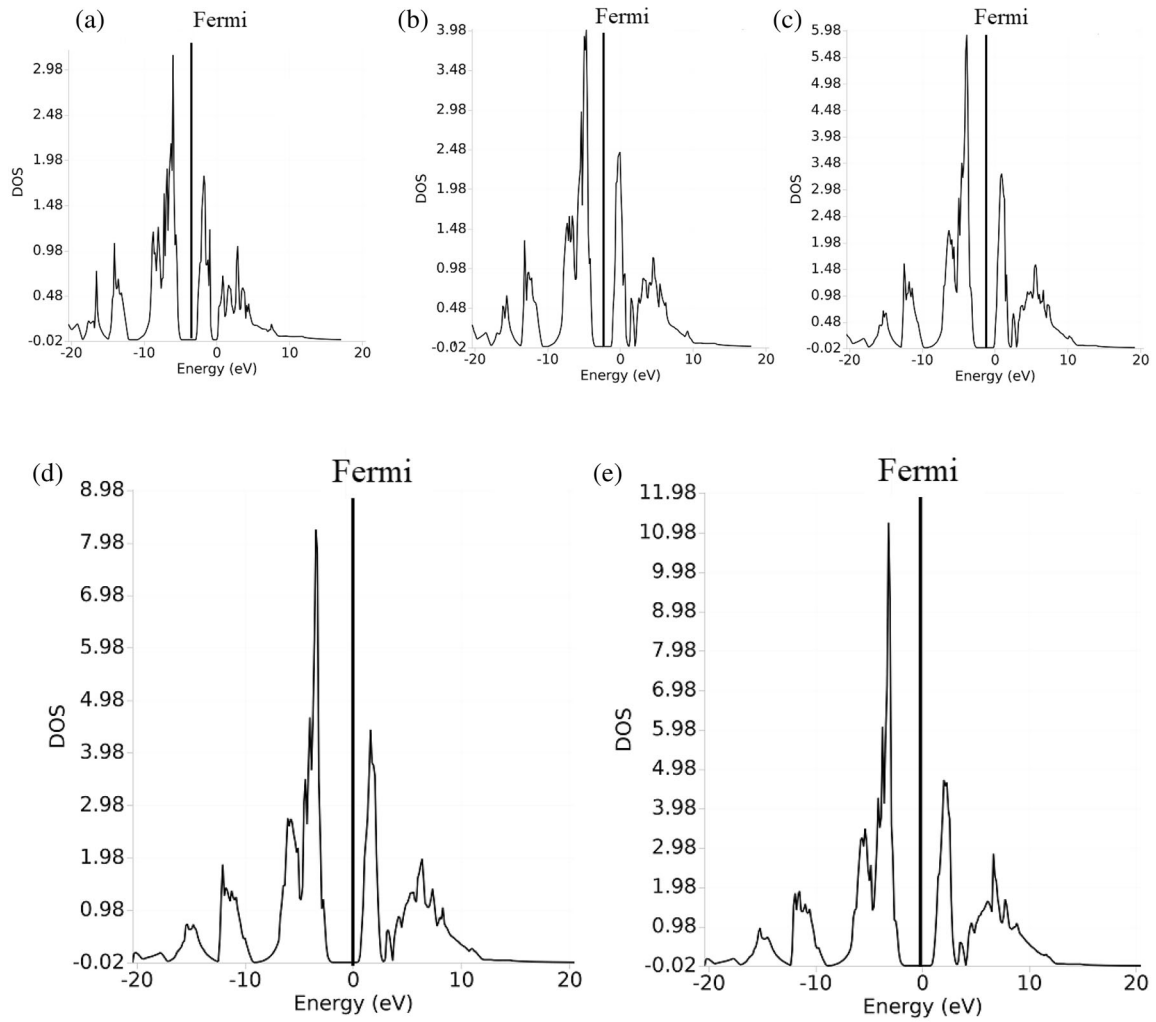

Figure 3. Total DOS of slab $PbTiO_3$: (**a**) slab $n = 2$ layer, (**b**) slab $n = 3$ layer, (**c**) slab $n = 4$ layer, (**d**) slab $n = 5$ layer and (**e**) slab $n = 6$ layer.

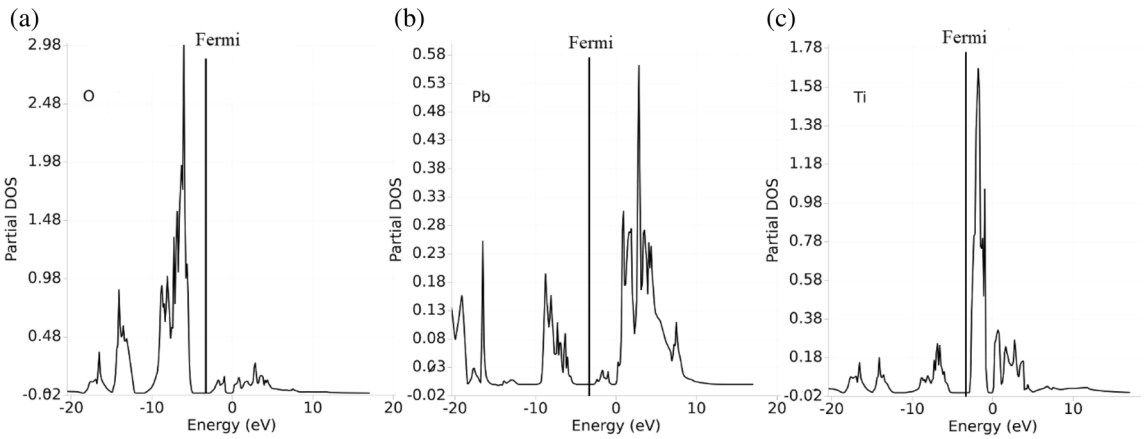

Figure 4. Partial DOS of slab $PbTiO_3$ for $n = 2$ layer: (**a**) O contribution, (**b**) Pb contribution and (**c**) Ti contribution.

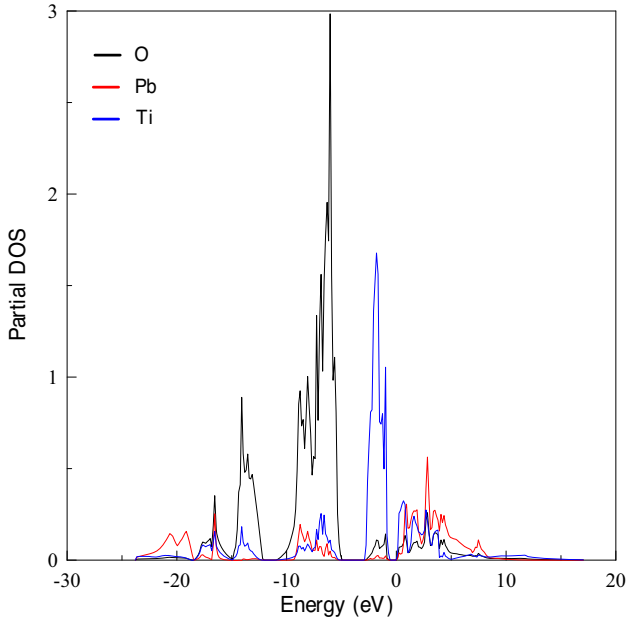

Figure 5. Partial density of the state's contributions from O, Pb and Ti in a single figure for $n = 2$ layer.

for O, Pb and Ti with $n = 2$ layers is shown in figure 4. As seen from partial DOS curves for $n = 2$ layer, the valence band is primarily occupied by oxygen 2p-states due to the presence of rich surface O atoms at the first peak, which is close to the Fermi level and a small amount of Pb 6p states. Above Fermi level, the band consists of dominantly Ti-3d states and Pb-5d states. The partial density of the state's contributions from O, Pb and Ti is plotted in a single picture to understand their difference, as seen in figure 5.

Figure 6a shows the variations of the bandgap with layers of slab from $n = 2$ to $n = 6$. The bandgap value of the slab is lower than the bulk structure. It can be said that there is a fast increase in the bandgap with the number of layer changes from 2 to 4, and the rate of increment decreases slightly when the number of layers is further increased. These results are consistent with periodic quantum-mechanical calculations based on the DFT of PbTiO3 slabs investigated by Lazaro *et al* [17].

The surface formation energies per surface area of slab $PbTiO_3$ with different layers are important to analyse stability. This energy is obtained to the total surface area of the slab by using the following equation:

$$E_{\text{formation}} = (E_{\text{slab}} - E_{\text{bulk}})/2A, \quad (3)$$

where E_{slab} is the total energy of slab with layers and A is the surface area of the slab, E_{bulk} represents the energy of the bulk systems containing the same number of molecular units as the slab [28]. The variation of formation energies with the number of layers of slab $PbTiO_3$ is plotted in figure 6b. There is no great variation in formation energy with the number of layer changes from 2 to 5, but a dramatically increment in formation energy occurs at the last layer due to less energetically stable surfaces. It can be also said that the first layered structure of the slab is more stable than the final slab structure. The surface formation energy depends significantly on the layers of the slab and it comes from the intrinsic properties of the materials.

4. Conclusions

The electronic properties of the bulk and slab including five layers in the range of $n = 2$–6 with (0 0 1) surface of $PbTiO_3$ have been investigated by employing extended TB self-consistent charge calculations based on DFT. The

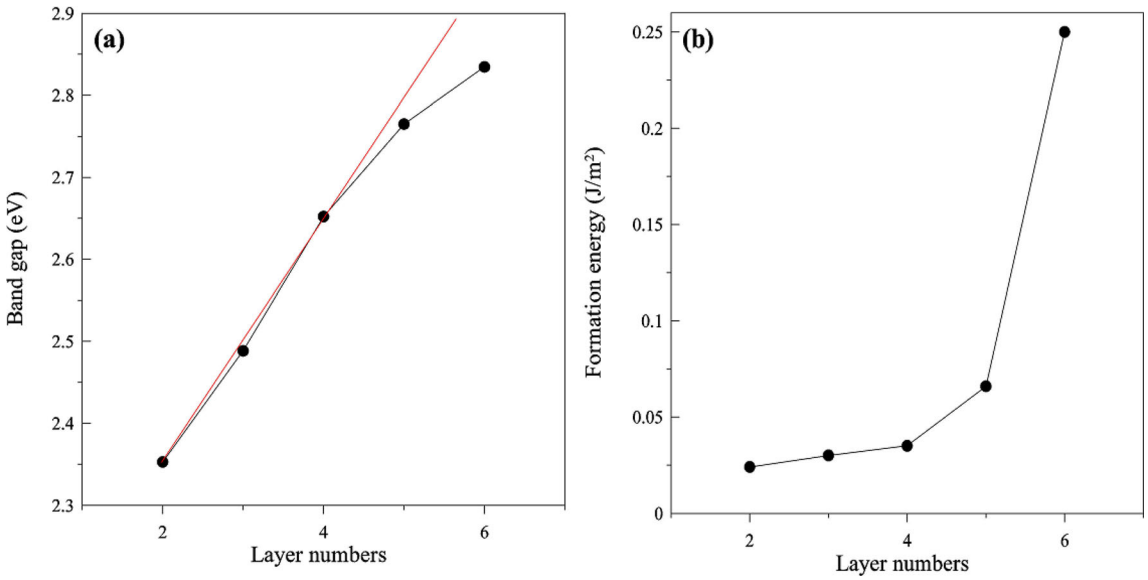

Figure 6. Variation of some parameters of slab $PbTiO_3$ with the number of layers: (**a**) bandgap and (**b**) formation energy.

bandgap of bulk $PbTiO_3$ is calculated as 4.3 eV along with the high symmetry directions. This result is in agreement with the experimental data. It is seen that the peaks of DOS increase with increasing layers of slab $PbTiO_3$ and the electronic contribution to DOS increase when the atom numbers increase in the slab. Moreover, it can be said that the bandgap and surface formation energy of slab $PbTiO_3$ increase with the number of layers from 2 to 6.

References

[1] Alam N N, Malik N A, Samat M H, Hussin N H, Jaafar N K, Radzwan A *et al* 2021 *Surf. Interfaces* **27** 101524

[2] Noor N A, Mahmood Q, Rashid M, Haq B U, Laref A and Ahmad S A 2018 *J. Solid State Chem.* **263** 115

[3] Eglitis R I, Purans J and Jia R 2021 *Cryst.* **11** 455

[4] Piskunov S, Heifets E, Eglitis R I and Borstel G 2004 *Comput. Mater. Sci.* **29** 165

[5] Eglitis R I 2009 *Integr. Ferroelectr.* **108** 11

[6] Piskunov S, Kotomin E A and Heifets E 2005 *Microelectron. Eng.* **81** 472

[7] Meyer B, Padilla J and Vanderbilt D 1999 *Faraday Disc.* **114** 395

[8] Noguchi Y 2021 *J. Ceram. Soc. Jpn.* **129** 271

[9] Munkholm A, Streiffer S K, Murty M R, Eastman J A, Thompson C, Auciello O *et al* 2001 *Phys. Rev. Lett.* **88** 016101

[10] Tasleem S and Tahir M 2020 *Renew. Sust. Energ. Rev.* **132** 110073

[11] Leite E R, Santos L P S, Carreno N L V, Longo E, Paskocimas C A, Varela J A *et al* 2001 *Appl. Phys. Lett.* **78** 2148

[12] Heifets E, Eglitis R I, Kotomin E A, Maier J and Borstel G 2001 *Phys. Rev. B* **64** 235417

[13] Shimada T, Tomoda S and Kitamura T 2009 *Phys. Rev. B* **79** 024102

[14] Eglitis R I, Piskunov S, Heifets E, Kotomin E A and Borstel G 2004 *Ceram. Int.* **30** 1989

[15] Eglitis R I and Vanderbilt D 2008 *Phys. Rev. B* **77** 195408

[16] Zhang J M, Pang Q, Xu K W and Ji V 2009 *Comput. Mater. Sci.* **44** 1360

[17] Lazaro S, Longo E, Sambrano J R and Beltrán A 2004 *Surf. Sci.* **552** 149

[18] Goh E S, Ong L H, Yoon T L and Chew K H 2016 *Curr. Appl. Phys.* **16** 1491

[19] Liu H, Seifert G and Di Valentin C 2019 *J. Chem. Phys.* **150** 094703

[20] Grimme S, Bannwarth C and Shushkov P 2017 *J. Chem. Theory Comput.* **13** 1989

[21] Bursch M, Neugebauer H and Grimme S 2019 *Angew. Chem. Int. Ed.* **58** 11078

[22] Kohn W and Sham L J 1965 *Phys. Rev.* **140** A1133

[23] Oliveira A F, Seifert G, Heine T and Duarte H A 2009 *J. Braz. Chem. Soc.* **20** 1193

[24] Vicent-Luna J M, Apergi S and Tao S 2021 *J Chem. Inf. Model.* **61** 4415

[25] Te Velde G T, Bickelhaupt F M, Baerends E J, Fonseca Guerra C, van Gisbergen S J A, Snijders J G *et al* 2001 *J. Comput. Chem.* **22** 931

[26] Fonseca Guerra C, Snijders J G, te Velde G and Baerends E J 1998 *Theor. Chem. Acc.* **99** 391

[27] Rüger R, Yakovlev A, Philipsen P, Borini S, Melix P, Oliveira A F *et al* 2013 *AMS DFTB 2021.1*, SCM, *Theoretical Chemistry* (Amsterdam, The Netherlands: Vrije Universiteit)

[28] Tao S X, Notten P H, van Santen R A and Jansen A P 2011 *Comput. Mater. Sci.* **50** 2960